The Virtual Admittance Control of Sending End Converter for Offshore Wind Farm Integration

Zhekai Li
Department of Electrical Engineering
Shanghai Jiao Tong University
Shanghai, China
zhekai_li.work@sjtu.edu.cn

Liliuyuan Liang
Contemporary Amperex Technology Co., Limited
Ningde, Fujian, China
LiangLLY@catl.com

Renxin Yang
Department of Electrical Engineering
Shanghai Jiao Tong University
Shanghai, China
frank_yang@sjtu.edu.cn

Xu Cai
Department of Electrical Engineering
Shanghai Jiao Tong University
Shanghai, China
xucai@sjtu.edu.cn

Abstract—In the voltage source converter-based high voltage direct current (VSC-HVDC) system with offshore wind farm (OWF) integration, the sending end converter (SEC) needs to operate in V/f controlling mode to provide stable AC voltage and frequency for the OWF. At present, the SEC mainly adopts the dual closed-loop control, i.e., the outer AC voltage loop and inner AC current loop. However, this control structure may suffer from coupling problems when applied in the modular multilevel converter (MMC) due to the absence of the AC-side filtering capacitor. Therefore, a virtual admittance-based control strategy is proposed in this paper to enhance the steady-state and dynamic control performance of the SEC. The small signal stability and the parameter design of the proposed method are introduced in this paper as well. Finally, the performance of the proposed control strategy is compared with the conventional dual closed-loop control in PSCAD/EMTDC. The simulation results show the effectiveness of the proposed control strategy.

Keywords—VSC-HVDC, MMC, wind farm, Sending end converter, Virtual admittance control

I. INTRODUCTION

To integrate and transfer bulk offshore wind power to the onshore grid, the voltage source converter-based high voltage direct current (VSC-HVDC) transmission system is becoming a promising alternative compared to its conventional HVAC counterpart [1]. To ensure the stable operation of offshore wind farms (OWFs), the sending end converter (SEC) of the VSC-HVDC system usually adopts constant voltage and frequency (V/f) control [2]. Besides, considering the low overcurrent capability of the power electronic devices, the inner current loop is added to constrain the fault current. Such AC-voltage AC-current dual closed-loop control is widely utilized in the SEC.

However, the conventional dual closed-loop structure is developed based on the 2-level VSC, which needs to obtain the feedforward of the output current and decoupling terms through the filter capacitor on the AC side. As for the modular multilevel converter (MMC), which is commonly used in high-voltage applications, there is no filter capacitor on the AC side [3][4]. The absence of the feedforward and decoupling terms may lead to stability problems [5] and control deterioration [6].
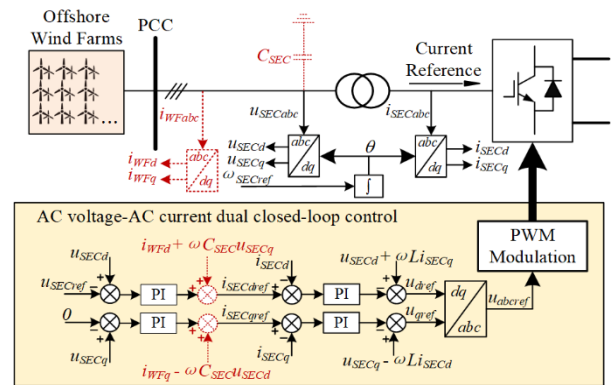
Fig. 1. Dual closed-loop control of the SEC

To solve the mentioned problems, a novel control strategy for SEC based on the virtual admittance principle is proposed in this paper. The virtual admittance link is utilized to replace the AC voltage control loop. In addition, the small signal stability and the parameter design of the proposed method are introduced. The simulations are conducted in PSCAD/EMTDC to verify the effectiveness of the proposed control strategy.

II. CONVENTIONAL DUAL CLOSED-LOOP CONTROL SCHEME

The conventional dual closed-loop control structure of the SEC is shown in Fig. 1. The V/f outer loop and inner current loop are utilized to constitute the control structure. The red dotted line shows the current feedforward and decoupling terms, which are obtained from the filter capacitor. In 2-level VSC, the voltage at the point of common coupling (PCC) can be written as:

$$u_{\text{SEC}} = \frac{1}{sC_{\text{SEC}}}\left(i_{\text{WF}} - i_{\text{SEC}}\right) \tag{1}$$

Therefore, the outer voltage loop can be decoupled from the inner current loop using the input current feedforward i_{WF}. However, these current feedforward terms are lost in MMC due to the absence of the filter capacitor. In this situation, the outer voltage loop and the inner current loop are no longer decoupled, leading to a worsened control performance. Moreover, the saturation of the outer loop is prone to occur under fault conditions, making its transient performance even worse.
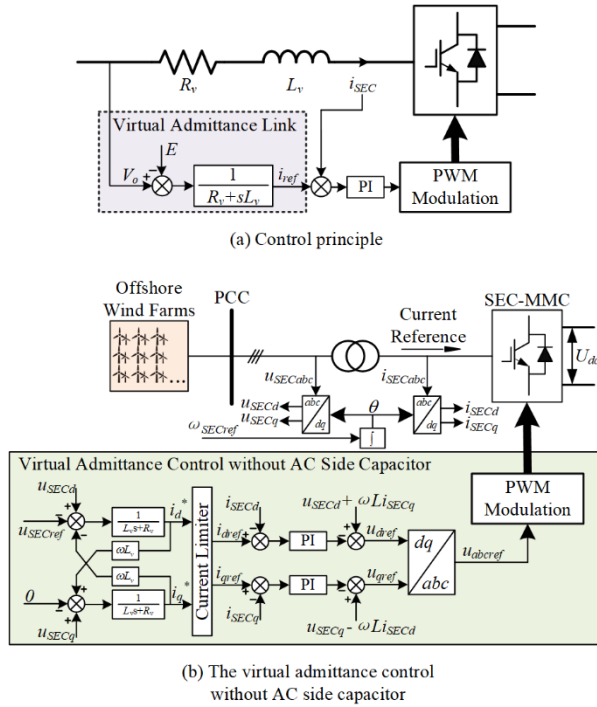
(a) Control principle

(b) The virtual admittance control
without AC side capacitor
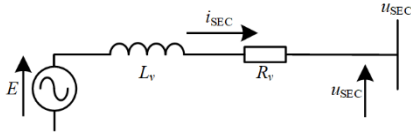
Fig. 2. Virtual admittance control scheme

Fig. 3. Simplified simulation of the output impedance of synchronous generator

III. VIRTUAL ADMITTANCE CONTROL OF SEC

As mentioned earlier, the absence of the filter capacitor makes it difficult to distinguish the wind farm current i_{WF} from the input current of the converter i_{SEC}. To solve this problem, the virtual admittance-based control scheme for SEC is proposed in this paper as shown in Fig. 2(b). The principle of virtual admittance control is shown in Fig. 2(a). The current reference is calculated by imitating the equation of the synchronous motor:

$$i_{SECref} = \frac{1}{R_v + sL_v}\left(u_{SEC} - E\right) \tag{2}$$

where E is the simulated "electromotive force" and u_{SEC} is the simulated "terminal voltage" of the motor. R_v and L_v are the virtual resistance and inductance, respectively. The simplified simulation of the output impedance of the synchronous machine is shown in Fig. 3. By controlling the input current to the same as i_{SECref}, E, namely voltage reference u_{SECref}, can be controlled to be a constant. However, the voltage drops on R_v and L_v will bring steady-state error to u_{SEC}, especially when the input current from the wind farm changes. Therefore, a PI controller, which is relatively slower, can be utilized to regulate u_{SEC} to the reference value by changing u_{SECref} or u_{abcref}. In addition, an elliptic current

limiter can be used to limit the given reference value i_{ref} to prevent the system from overcurrent, achieving the adaptive adjustment of the virtual admittance parameter. The design of the elliptic current limiter is shown as follows:

$$i_{dref} = \begin{cases} i_d^* & \sqrt{i_d^{*2} + i_q^{*2}} < i_{lim} \\ \dfrac{i_{lim}}{\sqrt{i_d^{*2} + i_q^{*2}}} i_d^* & \sqrt{i_d^{*2} + i_q^{*2}} \geq i_{lim} \end{cases} \tag{3}$$

$$i_{qref} = \begin{cases} i_q^* & \sqrt{i_d^{*2} + i_q^{*2}} < i_{lim} \\ \dfrac{i_{lim}}{\sqrt{i_d^{*2} + i_q^{*2}}} i_q^* & \sqrt{i_d^{*2} + i_q^{*2}} \geq i_{lim} \end{cases} \tag{4}$$

Different from the dual closed-loop control, the control based on virtual admittance does not require the load current feedforward provided by the filter capacitor, which makes this control have good performance and low design difficulty in the MMC converter topology. Moreover, its excellent dynamic current limitation ability makes the dynamic performance of the whole system significantly improved under the fault conditions such as low voltage ride-through (LVRT).

IV. PARAMETER DESIGN AND STABILITY ANALYSIS

The parameter design of the proposed control system consists of two parts, containing the inner current loop design and the virtual admittance outer loop design. The former is just the same as the traditional current inner loop design method [7]. The latter design and the stability analysis of the proposed control system are introduced as follows.

The complete system framework of SEC based on virtual admittance is shown in Fig. 2 (b). After linearizing the system through control equations and circuit equations, the following state-space equations can be constructed:

$$\Delta \dot{x} = A\Delta x + B\Delta u \tag{5}$$

The eigenvalues of the control system can be obtained by solving the state space matrix $\mathbf{A}$. It can be seen in Fig. 4(a) that all the eigenvalues are distributed in the left half plane (LHP), indicating that the built system is stable. Among all the eigenvalues, eigenvalues 1 and 2 are non-dominant poles far away from the imaginary axis. Therefore, eigenvalues 3~8 will be mainly analyzed.

To reflect the influence of virtual admittance parameters on the distribution of the eigenvalues, L_v and R_v were gradually changed from 0.03pu and 0.01pu to 0.3pu and 0.1pu. Fig. 4(b) shows that with the increase of L_v and R_v, eigenvalues cross the virtual axis from the right half plane (RHP) into the LHP, making the system stable. However, as for the values of L_v and R_v, bigger is not always better. Further verification is carried out by simulation.
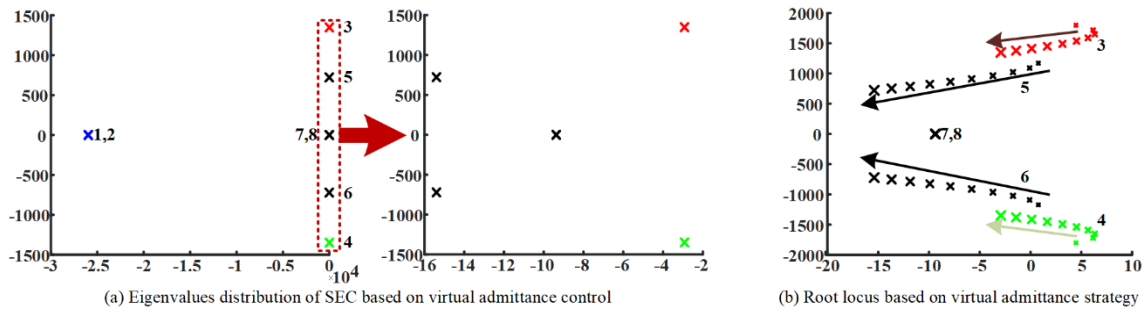
(a) Eigenvalues distribution of SEC based on virtual admittance control   (b) Root locus based on virtual admittance strategy

Fig. 4. Eigenvalues analysis of SEC based on virtual admittance control strategy

(a) L_v=0.03pu, R_v=0.01pu   (b) L_v=0.3pu, R_v=0.1pu   (c) L_v=3pu, R_v=1pu
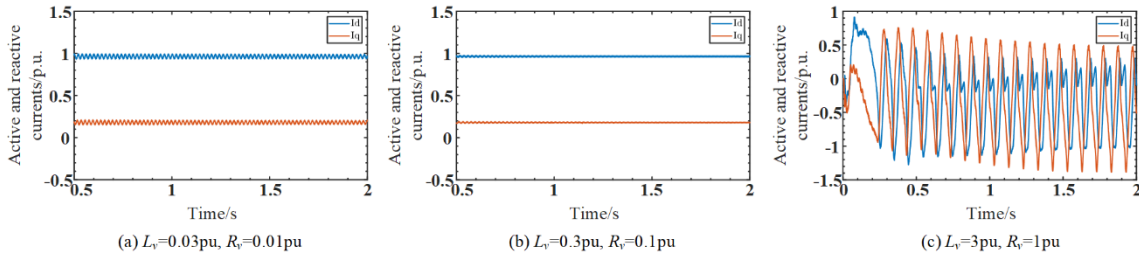
Fig. 5. Simulation verification when the virtual admittance parameter changes

According to the simulation results shown in Fig. 5, the decrease of L_v and R_v will deteriorate the system's dynamic performance and control stability. Whereas, although the increase of L_v and R_v can improve the dynamic control performance, it also reduces the active power transmission limit of the system and increase the risk of system instability. Therefore, considering both the stability margin and control performance, this paper takes the values of L_v and R_v to be 0.3pu and 0.1pu respectively.

V. SIMULATION SYSTEM AND RESULT

To verify the feasibility and superiority of the optimized control strategy based on the principle of virtual admittance, the simulations based on PSCAD/EMTDC are conducted under the practical engineering parameters of 1100MW/±400kV. The complete structure of the MMC-HVDC system with OWF integration is shown in Fig. 6 and the system parameters shown in Table I are taken to run the simulation.

The sudden change of the wind farm power and the wind farm AC voltage are two typical transient conditions in the operation of the offshore wind power system connected with MMC-HVDC. When the sudden change in the wind farm power

and the wind farm AC voltage happens, Fig. 7 shows the transient time domain waveform comparison of different control methods.

TABLE I.   PARAMETERS OF AGGREGATION WIND FARM AND MMC-HVDC SYSTEM

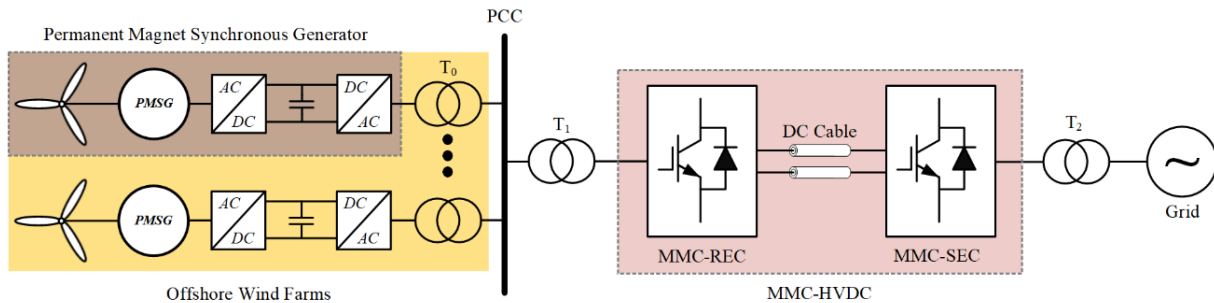| System parameters	Value
Rated AC voltage of the wind farm (kV)	0.69
Rated DC voltage of the wind farm (kV)	1.2
AC grid voltage (kV)	525
Rated AC voltage of the MMC (kV)	416
Rated DC voltage of the MMC (kV)	±400
Rated system capacity (MVA)	1100
Number of submodules	400
Arm inductance of MMC bridge (mH)	133
The capacitance of the submodule (mF)	11

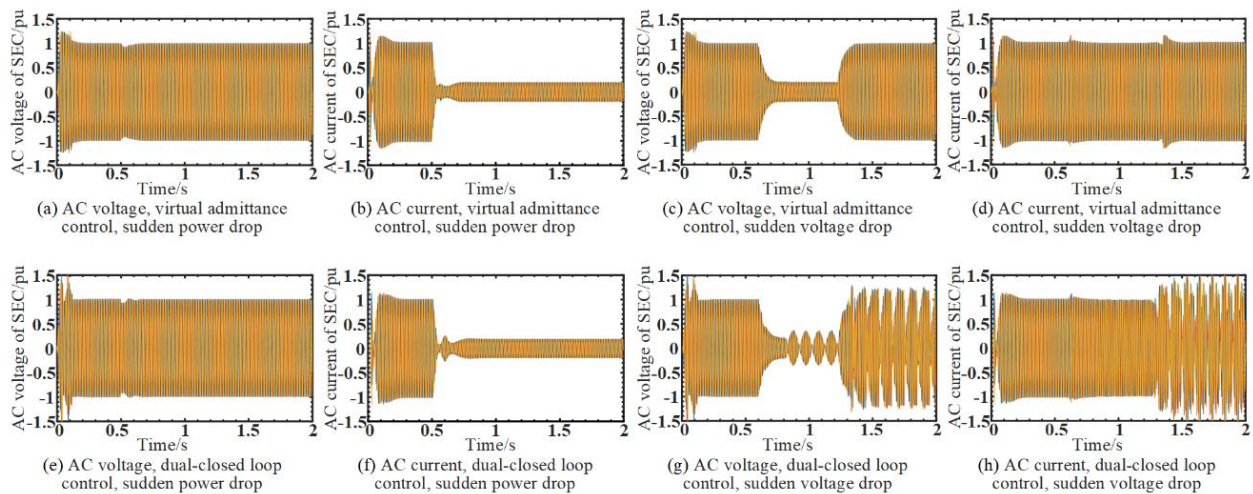Fig. 6. Diagram of offshore wind power system connected with MMC-HVDC

Fig. 7. Simulation result of different control strategies under various operating conditions

As can be seen from the simulation results shown in Fig. 7, the control strategy based on the virtual admittance principle is superior to the dual closed-loop control no matter in the steady-state condition or the transient condition of power drop and voltage drop, with faster response, better control performance, and more stable transient characteristics.

VI. CONCLUSION

The AC voltage-AC current dual closed-loop control commonly used in engineering has some defects in parameter adjustment and dual-loop coupling problems when applied to MMC without the AC filter capacitor. For the purpose of optimizing the steady-state and transient control performance of SEC, an optimized control strategy based on the virtual admittance principle is proposed in this paper, and the conclusions are gained as follows.

The proposed virtual admittance control strategy has excellent steady-state performance. Compared with the dual closed-loop control, the virtual admittance control-based SEC can enter the new steady state more quickly without oscillation under the condition of a sudden drop in wind farm power and only produce the transient voltage peak of 1.25pu, which is much smaller than the dual closed-loop. Under the condition of active voltage drop of SEC, the proposed virtual admittance control strategy not only avoid the problems of losing the outer loop feedforward and decoupling terms, but also solves the problem caused by the saturation of the outer loop with its adaptive current limitation design. The transient responses of voltage and current are smooth and rapid, with the current being effectively limited.

REFERENCES

[1] Muyeen, S. M., Takahashi, R., & Tamura, J. (2010). Operation and Control of HVDC-Connected Offshore Wind Farm. IEEE Transactions on Sustainable Energy, 1(1), 30–37. https://doi.org/10.1109/TSTE.2010.2041561

[2] Rocabert, J., Luna, A., Blaabjerg, F., & Rodríguez, P. (2012). Control of Power Converters in AC Microgrids. IEEE Transactions on Power Electronics, 27(11), 4734–4749. https://doi.org/10.1109/TPEL.2012.2199334

[3] K. Sharifabadi, L. Harnefors, H.-P. Nee, S. Norrga, and R. Teodorescu, Design, Control and Application of Modular Multilevel Converters for HVDC Transmission Systems, 1st ed. Hoboken, NJ, USA: Wiley, 2016.

[4] Xu, L., Yao, L., & Sasse, C. (2007). Grid Integration of Large DFIG-Based Wind Farms Using VSC Transmission. IEEE Transactions on Power Systems, 22(3), 976–984. https://doi.org/10.1109/TPWRS.2007.901306

[5] Lin, H., Lyu, J., Zhai, D., Wang, Y., Tang, B., & Cai, X. (2021). COMPARATIVE ANALYSIS OF IMPACT OF WIND FARM SIDE MMC WITH DIFFERENT AC VOLTAGE CONTROL STRATEGIES ON THE STABILITY OF MMC-HVDC CONNECTED WIND FARM. The 10th Renewable Power Generation Conference (RPG 2021), 2021, 1039–1045. https://doi.org/10.1049/icp.2021.2272

[6] Freytes, J., Li, J., de Préville, G., & Thouvenin, M. (2021). Grid-Forming Control With Current Limitation for MMC Under Unbalanced Fault Ride-Through. IEEE Transactions on Power Delivery, 36(3), 1914–1916. https://doi.org/10.1109/TPWRD.2021.3053148

[7] Blaabjerg, F., Teodorescu, R., Liserre, M., & Timbus, A. V. (2006). Overview of Control and Grid Synchronization for Distributed Power Generation Systems. IEEE Transactions on Industrial Electronics, 53(5), 1398–1409. https://doi.org/10.1109/TIE.2006.881997